Environmental Science and Pollution Research
https://doi.org/10.1007/s11356-020-10913-x

RESEARCH ARTICLE

Bismuth oxide nanoparticles induce oxidative stress and apoptosis in human breast cancer cells

Ali Alamer[1] · Daoud Ali[2] · Saud Alarifi[2] · Abdullah Alkahtane[2] · Mohammed AL-Zharani[3] · Mohamed M. Abdel-Daim[2,4] · Gadah Albasher[2] · Rafa Almeer[2] · Nouf K. Al-Sultan[2] · Abdulaziz Almalik[1,5] · Ali H Alhasan[1,5] · Christos Stournaras[6] · Saquib Hasnain[7] · Saad Alkahtani[2]

Received: 28 April 2020 / Accepted: 17 September 2020

Abstract

Metal nanomaterials such as bismuth oxide nanoparticles (Bi_2O_3NPs) have been extensively used in cosmetics, dental materials, pulp capping, and biomedical imaging. There is little knowledge about the health risk of Bi_2O_3NPs in humans, which warrants a thorough toxicity investigation of Bi_2O_3NPs at the cellular level. In this experiment, we investigated the cytotoxic effect of Bi_2O_3NPs on human breast cancer (MCF-7) cells over 24 and 48 h. MCF-7 cells were exposed to Bi_2O_3NPs at varying doses (0.1, 0.5, 1.0, 5, 10, 20, 40 μg/mL) for 24 and 48 h. We assessed the toxicity of Bi_2O_3NPs by measuring its effect on the viability and oxidative stress biomarkers, e.g., GSH, SOD, and catalase in MCF-7 cells. The pro-apoptotic effects of Bi_2O_3NPs on MCF-7 cells were determined via evaluating dysfunction of mitochondrial membrane potential (MMP), caspase-3 activity, externalization of phosphatidylserine, and chromosome condensation. Furthermore, apoptotic cells were evaluated using 7-AAD fluorescence stain and Annexin V-FITC. Bi_2O_3NPs induced oxidative stress in MCF-7 cells in a time- and dose-dependent manner. Bi_2O_3NPs increased the rate of both necrotic cells and apoptotic cells. In addition, the blue fluorescence of MCF-7 cells with condensed chromatin was increased in a time- and dose-dependent manner. In conclusion, the present study highlights the potential toxic effects of Bi_2O_3NPs at the cellular level and suggests further investigation of Bi_2O_3NPs before any medical purposes.

Keywords Bi_2O_3NPs · MCF-7 cells · Cytotoxicity · Apoptosis

Responsible editor: Philippe Garrigues

✉ Saad Alkahtani
salkahtani@ksu.edu.sa

[1] National Center for Pharmaceutical Technology, King Abdulaziz City for Science and Technology, Riyadh, Saudi Arabia

[2] Department of Zoology, College of Science, King Saud University, Riyadh, Saudi Arabia

[3] Department of Biology, College of Science, Imam Muhammad Ibn Saud Islamic University, Riyadh, Saudi Arabia

[4] Pharmacology Department, Faculty of Veterinary Medicine, Suez Canal University, Ismailia 41522, Egypt

[5] National Center for Pharmaceuticals, Life science and Environment Research Institute, King Abdulaziz City for Science and Technology (KACST), Riyadh, Saudi Arabia

[6] Department of Biochemistry, University of Crete Medical School, Voutes, Greece

[7] Department of Pharmacy, Shri Venkateshwara University, Gajraula, Amroha, UP, India

Introduction

Cancer is the second leading cause of mortality after cardiovascular diseases worldwide (Kooti et al. 2017). In addition to genetic drivers, there are environmental factors that cause cancer (Doubeni et al. 2019). Breast cancer is the most common cancer in women under the age of 60. The rates of treatment success are high in the early stages with high survival rates. However, in advanced or late stages, the treatment is often insufficient, with a 5-year survival rate of less than 25% (Pradeepkumar and Kumar 2018). Breast cancer cell line (MCF-7) has been widely used as an in vitro model for breast cancer (Riaz et al. 2013). One example of MCF-7 contributions in breast cancer research is its utility for the study of the estrogen receptor (ER) alpha, as this cell line expresses substantial levels of ER mimicking the majority of invasive human breast cancers (Novaro et al. 2003; Alberts 2008).

Bismuth nanoparticles have attracted interest in health sciences (bioimaging, biosensing, biomolecular detection, and dental materials) and cosmetic industry owing to their

remarkable physico-chemical properties from nanoelectronics to catalysis (Hyodo et al. 2009; Patil et al. 2020). However, the toxicity of such nanoparticles at the molecular level has not been extensively explored, and it is a crucial step prior to biomedical applications. Some researchers have reported that metal nanomaterials can accumulate in different tissues, leading to toxic effects, such as oxidative stress and apoptosis (Karam et al. 2007; Chen et al. 2015). Bi_2O_3NPs induce toxicity in various mammalian cells (Ding et al. 2011; Abudayyak et al. 2017; Wang et al. 2017) by increasing the production of intracellular reactive oxygen species (ROS) at a rate that overwhelms the cellular defense mechanisms. High levels of ROS in cellular systems can lead to irreversible molecular damages of the genetic materials and organic compounds, resulting in cytotoxicity and genotoxicity (Finkel and Holbrook 2000; Valko et al. 2007).

Hence, it is of outmost importance to study the cellular toxicity of Bi_2O_3NPs prior to any translational medical application. Accounting for in vitro genotoxicity and cell apoptosis caused by Bi_2O_3NPs, the present study investigated the involvement of complex cellular responses via diverse biological processes compromised by Bi_2O_3NPs including cell viability, mitochondrial membrane dysfunction, oxidative stress–mediated apoptosis, and genotoxicity on human breast cancer (MCF-7) cell line.

Material and methods

Chemicals

Bismuth oxide nanopowder (Bi_2O_3NPs), < 10 nm particle size, 99% trace metal basis; 3-(4,5-dimethylthiozolyl-2)-2,5-diphenyl tetrazolium bromide (MTT); 2'-7'-dichlorodihydrofluorescein diacetate (DCFH-DA); acridine orange (AO); ethidium bromide (EtBr); phosphate buffer saline (PBS); propidium iodide; and Trypsin-EDTA solution were purchased from Thermo Fisher Life Technologies, USA. The caspase-3 assay kit and fetal bovine serum (FBS), Triton X-100, antibiotics (penicillin–streptomycin), and DMEM medium were purchased from Sigma-Aldrich, USA. The whole consumables and culture wares were procured from Corning, NY, USA.

Cell culture

MCF-7 cells (ATCC® HTB-22™) were seeded in DMEM supplemented with 10% FBS and 1.5% antibiotic solution. Cells were grown in standard conditions. Cells were observed with (Nikon Eclipse TE2000) an inverted microscope.

Treatments of Bi_2O_3NPs

MCF-7 cells were subcultured overnight before exposure to Bi_2O_3NPs (0, 0.1, 0.5, 5, 10, 20, 40, 100 μg/mL). Bi_2O_3NPs was suspended in 1 mg/mL DMEM medium and diluted to 0.1–100 μg/mL. Suspended solution of Bi_2O_3NPs was sonicated by using the Qsonica Q700 sonicator at 40 W at RT for 15 min to prevent aggregation of Bi_2O_3NPs.

Physiochemical characterization of Bi_2O_3NPs

A small amount of nanoparticles was smashed on a slide then inserted into the X-ray diffraction (XRD, Rigaku MiniFlex 600) to characterize crystallinity using CuKα radiation (30 kV, 40 mA, 1.54430 A°) between 5 and 80°. The morphology of Bi_2O_3NPs was measured using a scanning electron microscope (SEM).

Bi_2O_3NPs were suspended in DDW (100 μg/mL), and films of NPs on the transmission electron microscope (TEM) grid were prepared by dipping in NP suspension. The excess solution was removed by using a blotting paper. The size of Bi_2O_3NPs was determined by using TEM (JEM 1011, Japan) with a voltage of 80 kV.

To further measure the hydrodynamic diameters of Bi_2O_3NPs, Bi_2O_3NPs were sonicated using probe sonication. After sonication, Bi_2O_3NP suspension was added into a folded capillary cell (DTS1070), followed by dynamic light scattering (DLS) analysis using Zetasizer (ZEN3600, Malvern, UK) to measure Z-average hydrodynamic diameters, and zeta potential at room temperature.

MTT assay

The cytotoxicity of Bi_2O_3NPs on MCF-7 cells was assessed by using the MTT assay kit (Abcam, ab211091). MCF-7 cells were cultured in 96-wells plate and exposed to Bi_2O_3NPs (0, 0.1, 0.5, 5, 10, 20, 40, 100 μg/mL) for 24 and 48 h. After exposure to nanoparticles, the plate suspension was discarded. New MTT solution (0.5 mg/mL) in DMEM was added and incubated for 4 h. The formazan crystal was formed, and optical density was observed at 570 nm using a microplate reader (Multiskan® Ascent, LabSystems, and Haverhill, MA, USA).

ROS measurement

ROS were measured using 2,7-dichlorodihydrofluorescin diacetate (H2-DCFH-DA). H2-DCFH-DA was dissolved in dimethyl sulfoxide to 5 mM as an optimal concentration. A black well plate (96 wells) was used for treatment. The working solutions containing 10 μM H2-DCFH-DA were added to

MCF-7 cells and incubated for 30 min at 37 °C in duplicate. The cells were washed once with PBS and re-suspended in PBS. A spectro-fluorometer was used to measure the relative fluorescence intensity at 480-nm excitation wavelengths and 530-nm emission.

For assessment of the generated ROS, MCF-7 cells were incubated with Bi_2O_3NPs. The cells were incubated with H2-DCFH-DA (5 mM) at 37 °C for 30 min, then washed with PBS and fixed with paraformaldehyde (4%). The fluorescence of cells was measured by fluorescence microscope (Nikon Eclipse 80i).

Oxidative stress biomarkers

MCF-7 cells (6×10^6) was cultured in a 75-cm^2 flask and treated with various dose of Bi_2O_3NPs (1, 5, 10, 20, and 40 μg/mL) for 24 and 48 h. MCF-7 cells were washed with PBS and scraped. The scraped cells were incubated in lysis buffer (20 mM Tris-HCl [pH 7.5], 150 mM NaCl, 1 mM Na2 EDTA, 1% Triton, and 2.5 mM sodium pyrophosphate). MCF-7 cells were centrifuged at 15,000 rpm at 4 °C for 15 min. The supernatant was kept at – 80 °C in freezer to measure the oxidative stress biomarkers, such as glutathione (GSH), superoxide dismutase (SOD), and catalase. GSH was measured by using a GSH kit (item no. 703002, Cayman chemical). SOD was measured by using a SOD kit (item no. 706002, Cayman chemical), and catalase was measured by using a catalase kit (item no. 707002, Cayman chemical). Protein concentration was measured by using the Bradford method (1976).

JC-1 assay

The JC-1 assay was used to determine mitochondrial membrane potential (MMP) in MCF-7 cells after exposure to nanoparticles using the JC-1 assay kit (Cayman chemical kits), and the test was done according to manufacturer's instruction.

Examination of phosphatidylserine translocation

MCF-7 cells were cultured and incubated with Bi_2O_3NPs (5, 10, and 20 μg/mL) for 24 and 48 h. After incubation, the cells were fixed with paraformaldehyde (4%) for 5 min and then washed with cold PBS. Cells were stained with propidium iodide (10 μL/mL) and Annexin V/FITC conjugate (2 μL) in binding buffer (500 μL). The images were examined by using a confocal microscope with emission 520 nm and excitation 488 nm for Annexin V/FITC and emission 617 nm and excitation 536 nm for propidium iodide.

Measuring of chromosome condensation and caspase-3 activity

The chromatin condensation was measured in treated MCF-7 cells after exposure to Bi_2O_3NPs (5, 10, and 20 μg/mL) for 24 and 48 h. Chromatin condensation was observed by DAPI staining. The condensed chromatin body in treated cells was detected according to Toné et al.'s (2007) method. In addition,

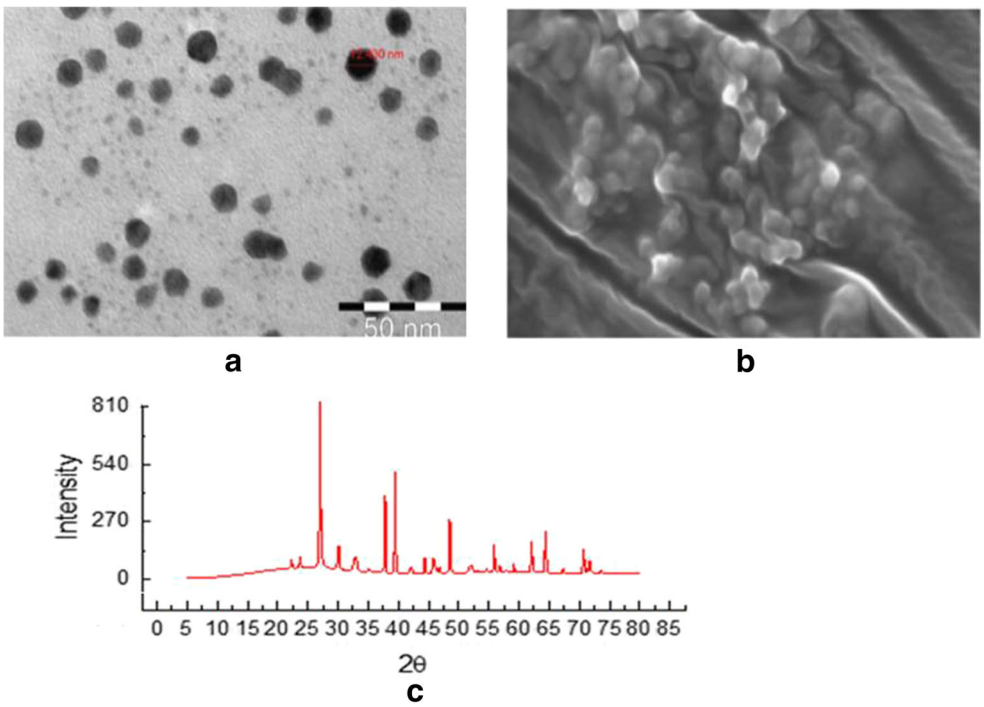

Fig. 1 **a** TEM image of Bi_2O_3NPs. **b** SEM image of Bi_2O_3NPs. **c** X-ray diffraction spectra of Bi_2O_3NPs

Table 1 The hydrodynamic size and zeta potential of Bi2O3NPs

Solvent	Dynamic light scattering
Size in water	470.5667 ± 40.22938
Zeta in water	− 22.6 ± 0.404145
Size in DEME	390.9333 ± 39.6437
Zeta in DEME	− 9.38667 ± 0.491155

the level of caspase-3 enzyme was measured in MCF-7 cells after treating with Bi_2O_3NPs for 24 and 48 h using Cayman Chemical colorimetric assay kits.

Annexin V-FITC/7-ADD staining

The Guava Nexin® assay was used to detect PS on the external membrane of apoptotic cells. The bismuth nanoparticles of different concentrations (5, 10, and 20 μg/mL) and final volume of 200 μL of triton (0.1% v/v) medium were used as positive control to detect PS in MCF-7 cells. Positive control was added to MCF-7 just 15–120 min before running the assay, then incubated for 24 and 48 h (5% CO_2 and 37 °C). The cell line was harvested at 85% confluence (5 × 104) by 0.25% trypsin in 96-well plates. The cells were directly stained in a 96-well microplate with Guava Nexin reagent, a pre-made cocktail containing Annexin V-PE and 7-AAD, in a

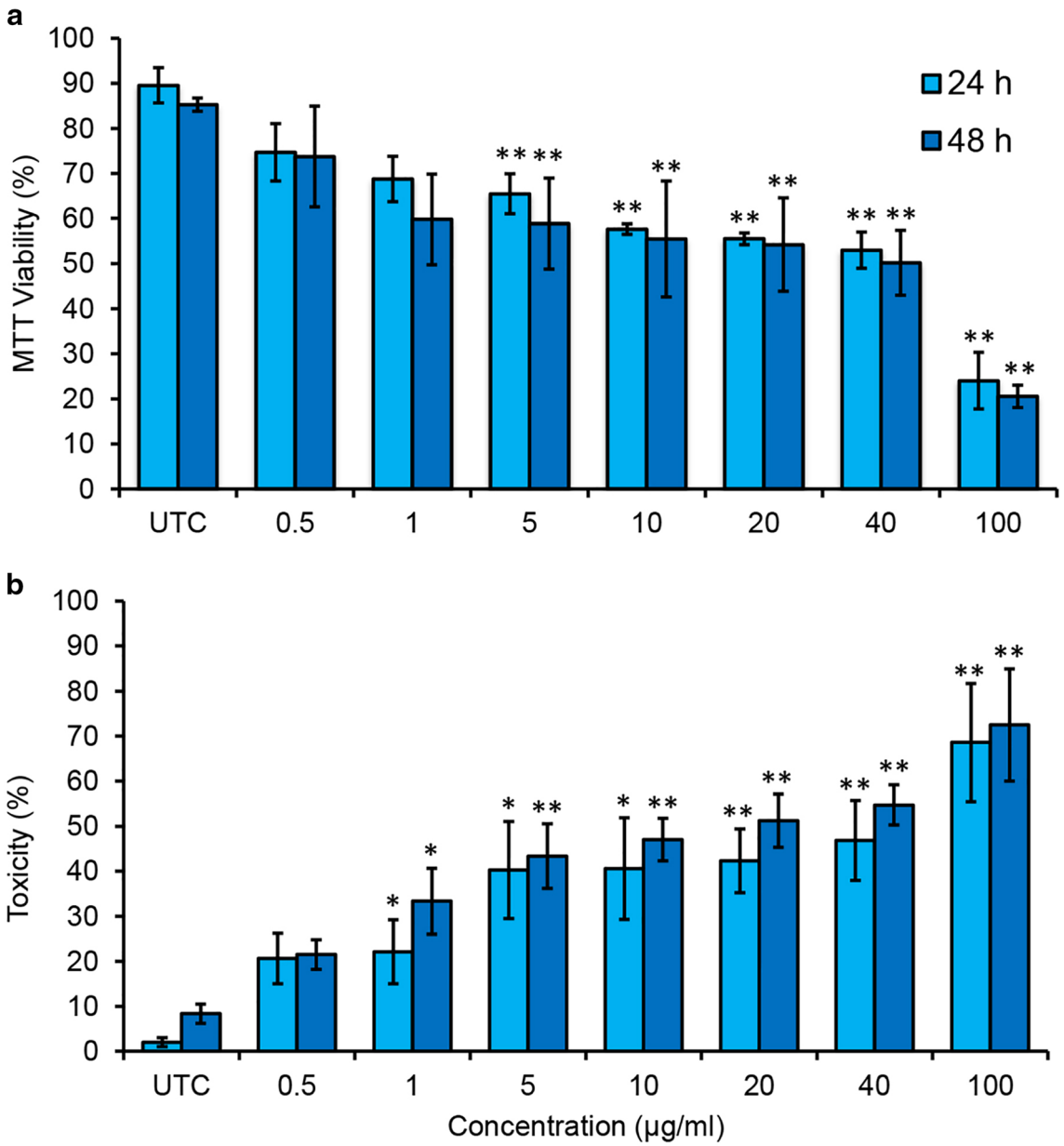

Fig. 2 Cytotoxicity of Bi_2O_3NPs on MCF-7 cells for 24 h and 48 h, as determined by **a** MTT tests and **b** LDH assay. Each value represents the mean ± SE of three experiments. *$p < 0.05$ and **$p < 0.01$ vs. control

200-μL final volume. After a 20-min incubation at room temperature, the samples were acquired on a Guava® System. Apoptosis assay was done according to manufacturer's instructions.

Statistical analysis

Pearson's correlation and one-way analysis of variance (ANOVA) were used to analyze the parametric data using the SPSS software version 26.0 (IBM company, USA). The difference between the results was considered slightly significant at $*p < 0.05$ and highly significant at $**p < 0.01$. Data was expressed as average value of triplicate independent experiment.

Results

Physical characterization of Bi_2O_3NPs

The shape, surface, size, and area of investigated nanoparticles were examined by TEM and SEM. The average size of Bi_2O_3NPs was 14 ± 11 nm by TEM (Fig. 1a). The SEM image shows that the powder of Bi_2O_3NPs is strongly agglomerated. The surface charge density of Bi_2O_3NPs in culture media suspension was determined by DLS with a zeta potential of − 22.6 ± 0.4 mV (Table 1). XRD analysis showed the high crystallinity of Bi_2O_3NPs (Fig. 1c). The estimated size of NPs as measured by XRD was 14 ± 7 nm, which is comparable to the TEM results in Fig. 1a.

Cytotoxicity

The viability of MCF-7 cells was evaluated after treatment with different doses (0.1, 0.5, 1, 5, 10, 20, 40, and 100 μg/mL) of Bi_2O_3NPs for 24- and 48-h incubation time using two methods (MTT and LDH assays). Pronounced dose-dependent response of cells was observed as suggested by the loss of cell survival as a result of elevation in the concentration of nanoparticles (Fig. 2a). The data of LDH assay were accorded with the MTT test (Fig. 2b). Thus, it is clear that Bi_2O_3NPs induced cytotoxic effects in a concentration- and time-dependent manner (Fig. 2). The cytotoxicity was more pronounced when exposing cells to 5 μg/mL of Bi_2O_3NPs and

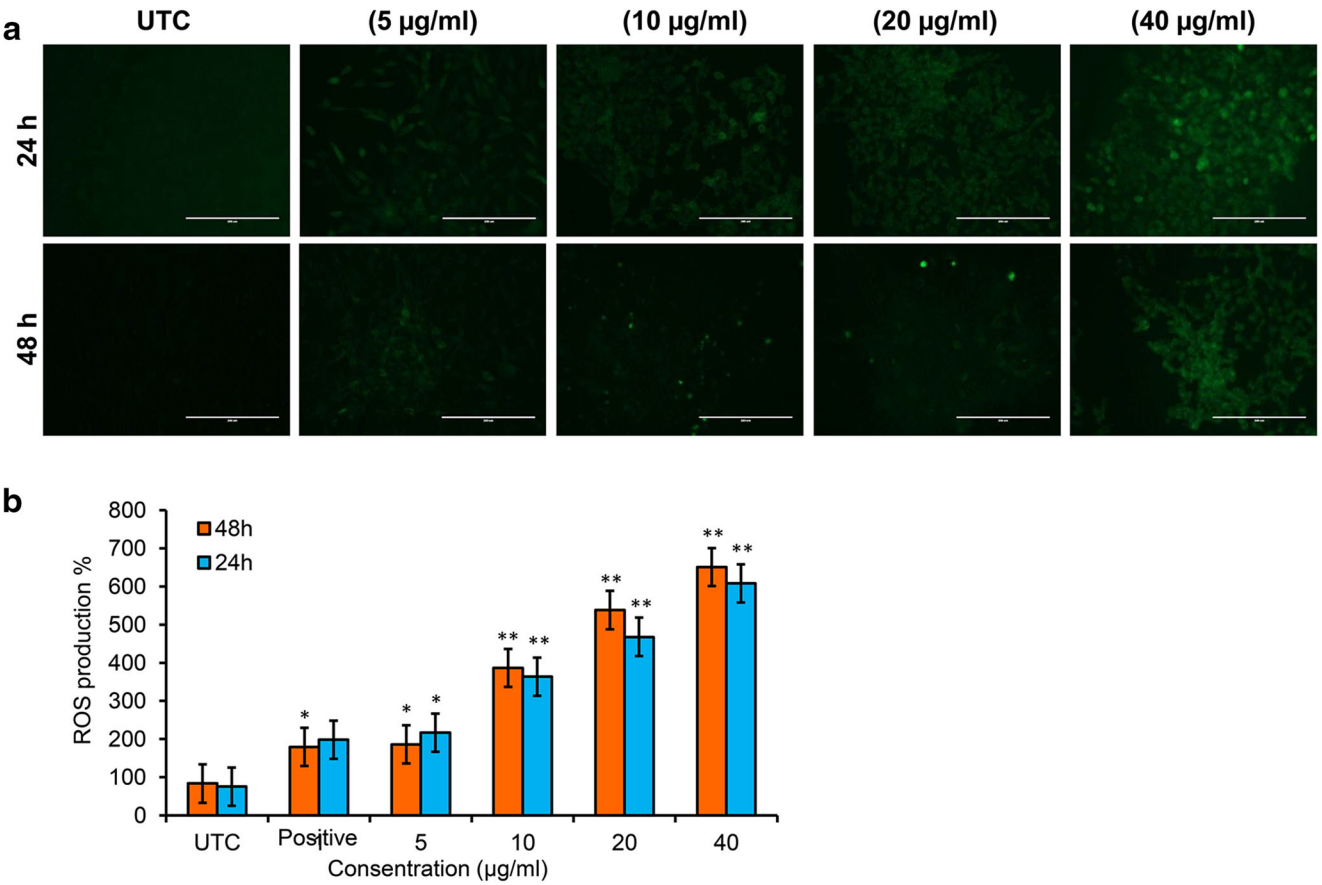

Fig. 3 Generation of ROS due to Bi_2O_3NPs. **a** The fluorescence image of MCF-7 cells treated for 24 h and 48 h and stained with DCFH-DA. **b** % ROS production due to Bi_2O_3NPs in MCF-7 cells. Each value represents the mean ± SE of three experiments. $*p < 0.05$ and $**p < 0.01$ vs. control

beyond; therefore, we limited our further toxicity studies to the high concentrations of Bi_2O_3NPs.

Oxidative stress

Intracellular ROS were measured using DCFDA fluorescent dye after incubating MCF-7 cells with Bi_2O_3NPs for 24 and 48 h. ROS generation was significantly increased (Fig. 3 a and b). The higher the concentration of Bi_2O_3NPs, the more significant the stress was on MCF-7 cells at the two time points. Glutathione reductase was increased up to 43%, 84%, and 96% in 24 h (Fig. 4a), and 41%, 80%, and 83% in 48 h (Fig. 4b) post-exposure to 5, 10, and 20 μg/mL of Bi_2O_3NPs, respectively.

The activity of SOD enzyme decreased significantly from 100 down to 49% and 38% in 24 h and down to 61% and 9% in 48 h (Fig. 4d) at 10 and 20 μg/mL Bi_2O_3NPs exposure, respectively (Fig. 4 c, d). Furthermore, there was a significant increase in the catalase concentrations in MCF-7 cells following Bi_2O_3NPs exposure. The results showed that the catalase activity increased significantly ($p < 0.05$) up to 35%, 40.1%, 40%, and 56% in 24 h (Fig. 4e), and up to 63%, 70%, 82%, and 83% in 48 h (Fig. 4f) in cells incubated with 5, 10, 20, and 40 μg/mL Bi_2O_3NPs, respectively.

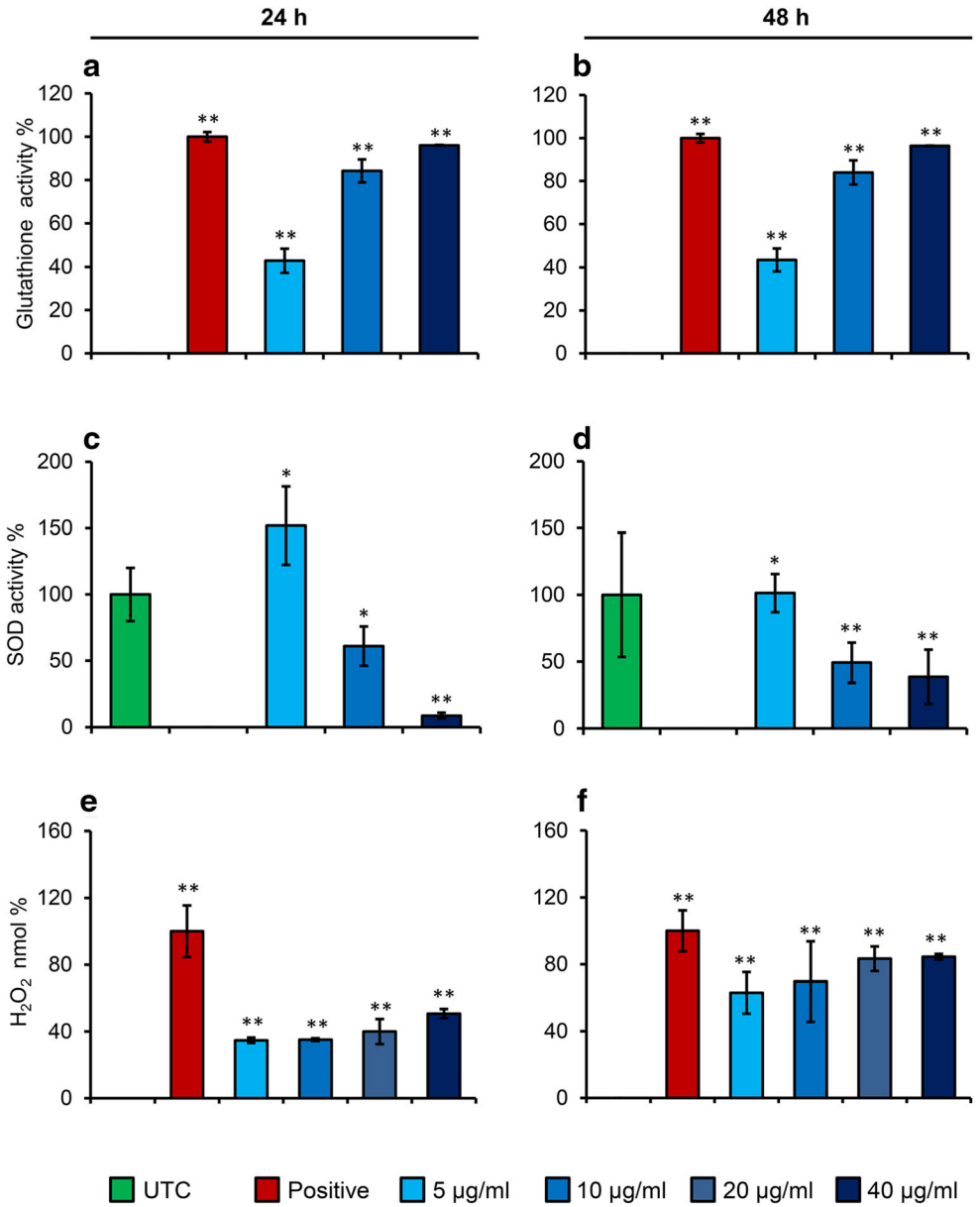

Fig. 4 **a** Levels of GSH in 24 h. **b** GSH in 48 h. **c** SOD in 24 h. **d** SOD in 48 h. **e** Catalase in 24 h. **f** Catalase in 48 h in MCF-7 cells after exposure to Bi_2O_3NPs for 24 and 48 h. Each value represents the mean ± SE of three experiments. *$p < 0.05$ and **$p < 0.01$ vs. control

Mitochondrial membrane potential

After exposing MCF-7 cells to Bi_2O_3NPs, the lost MMP was evaluated by using the JC-1 fluorescent dye staining method. The strong MMP was observed in untreated cell as the JC-1 dye enters to cells and causes J aggregates with deep red fluorescence. On the other hand, MMP was compromised when cells were incubated with Bi_2O_3NPs, especially at higher concentrations and longer durations due to inability of the cells to incorporate JC-1 stain (Fig. 5a). Pearson correlation for JC-1 24 h (Fig. 5b) and 48 h post-incubations (Fig. 5c) indicated strong positive correlation of loss of MMP as a function of increasing the concentration of Bi_2O_3NPs at both incubation time points.

Apoptosis

The apoptotic effects of Bi_2O_3NPs in MCF-7 cells were confirmed using different parameters such as chromosome condensation, caspase-3 activity, phosphatidylserine translocation, and apoptotic and necrotic cell sorting by using a flow cytometer. Untreated (UTC) cells showed normal nucleus, whereas the apoptotic cells showed fragmented chromatin with blue color fluorescence (Fig. 6a). Moreover, the current result revealed significant upregulation of caspase-3 enzyme activity in treated cells as compared with untreated cells (Fig. 6b). Induction of caspase-3 enzyme activity led to cleavage of specific substrates which in turn led to cell death. Time- and dose-dependent effects were remarkably observed as caspase-3 activity increased from 57 to 74% and from 87 to 93% at 24- and 48-h incubation time points, respectively. The leakage of phosphatidylserine from treated MCF-7 cells is an indicator of early apoptosis (Fig. 7). The leakage of phosphatidylserine was significantly increased in a dose- and time-dependent manner. The percentage of apoptotic vs. necrotic cells after exposing was measured using Annexin V-FITC and 7-AAD fluorescent stains. Flow cytometry analysis revealed that Bi_2O_3NPs (20 μg/mL) induced apoptosis and necrosis as compared with control (Fig. 8a).

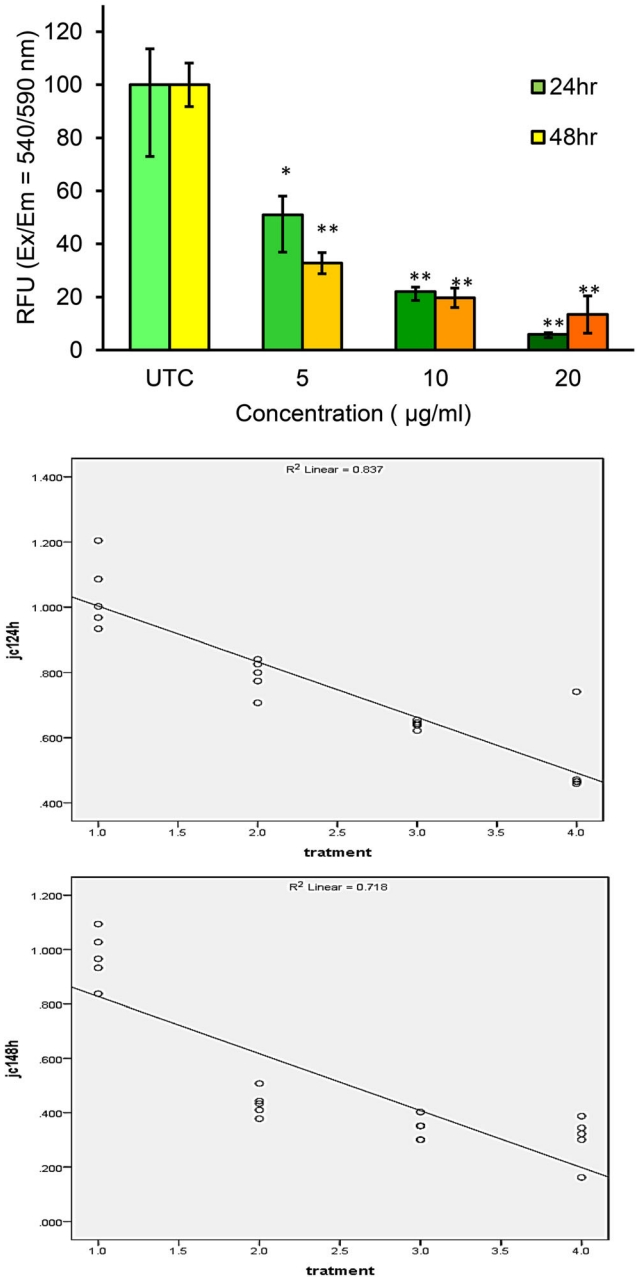

Fig. 5 a Loss of mitochondrial membrane potential determined due to Bi_2O_3NP exposure on MCF-7 cells for 24 h and 48 h, as determined by JC-1 fluorescence dye. b Pearson correlation of JC1 24 h. c Pearson correlation of JC1 48 h. *$p < 0.05$ and **$p < 0.01$ vs. control

Discussion

Few studies have reported on the hazardous effect of bismuth compounds. The toxicity of nano-sized bismuth oxide (Bi_2O_3NPs) differs from bismuth compound due to size, large surface area, and physiochemical nature. The present study was designed to investigate the cytotoxicity and apoptosis of Bi_2O_3NPs in MCF-7 cells. The size of Bi_2O_3NPs was 100 nm according to the supplier; however, the size and shape of nanoparticles were determined by SEM, TEM, and DLS. The measured size of Bi_2O_3NPs was more than the original (supplier) size. In comparison with measurements in the dry phase, the average particle sizes and size distributions of particles, measured by DLS, were enhanced when measured in aqueous media. Due to high specific surface area and energy level, nanoparticles have the propensity to form micro-size particles that are more stable in the environment (He et al. 2010). To protect the formation of agglomeration, the suspension of nanoparticles was prepared freshly and sonicated prior to the experiment. Strayer et al. (2015) reported that nanoparticles induced more toxic effects due their size, shape, and surface chemistry.

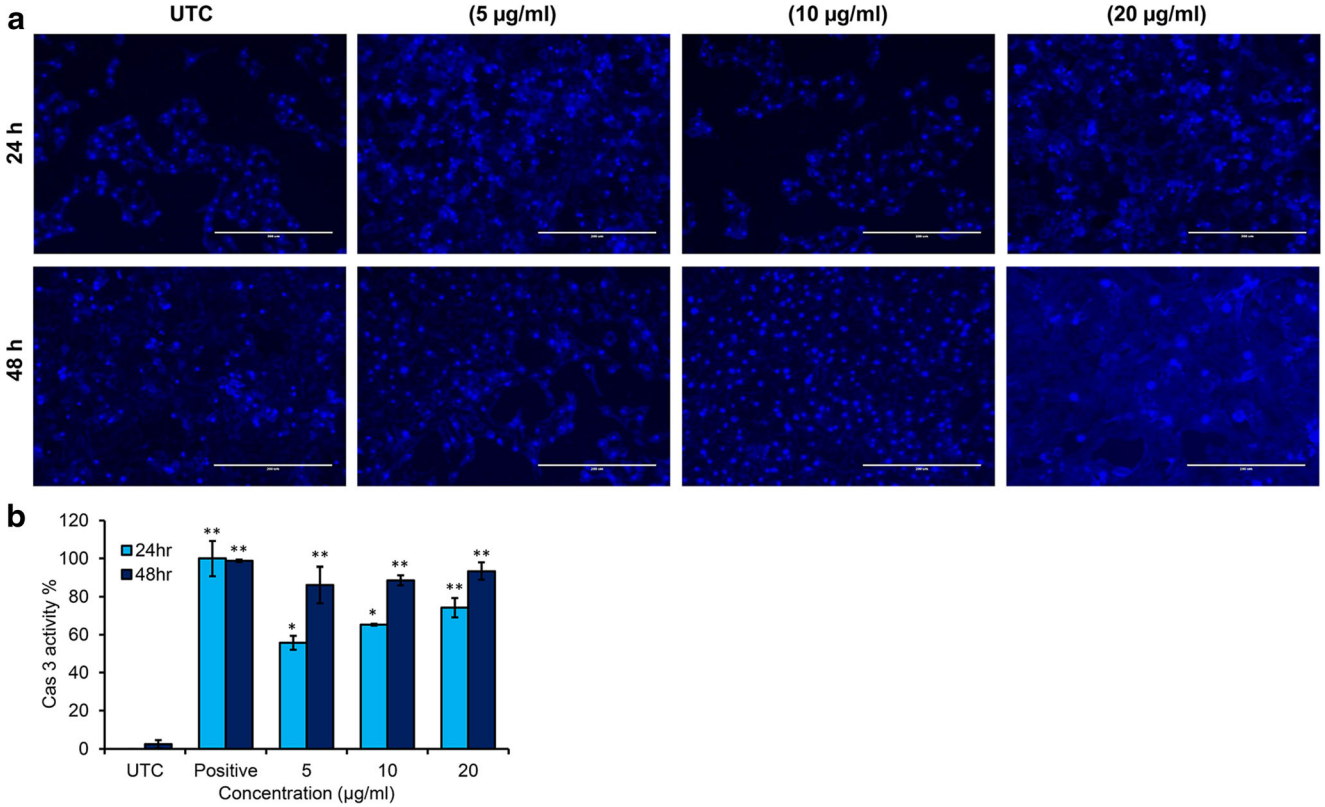

Fig. 6 **a** Chromosomal condensation in MCF-7 cells after exposure to nanoparticles for 24 to 48 h. **b** Induction of caspase-3 activity in MCF-7 cells after exposure to nanoparticle for 24 h and 48 h. Each value represents the mean ± SE of three experiments. *$p < 0.05$ and **$p < 0.01$ vs. control

In the current experiment, we aimed to identify the cytotoxic mechanism of Bi_2O_3NPs either necrosis or apoptosis in the dose- and time-dependent manner. Therefore, we performed MTT assay that targets mitochondrial function and the NRU assay that tested lysosomal activity in MCF-7 cells. Bi_2O_3NPs increased the caspase-3 activity and the

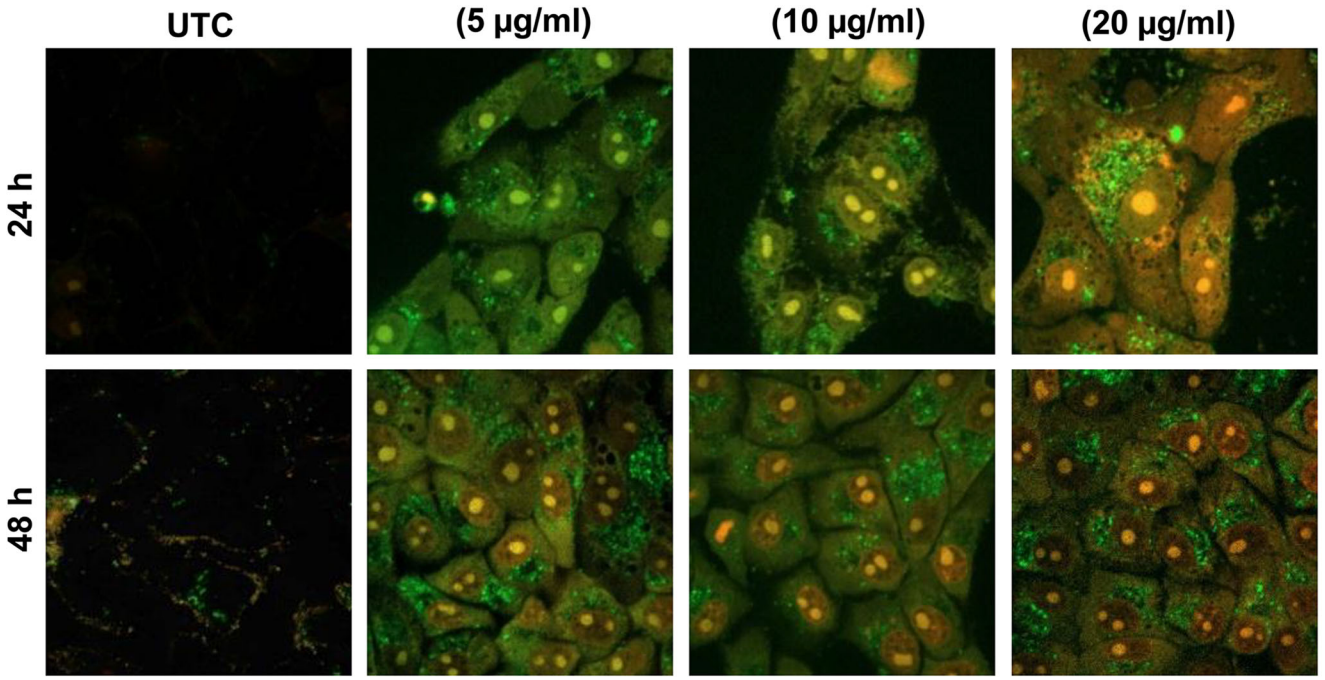

Fig. 7 Phosphatidylserine (PS) translocation in MCF-7 cells after exposure to various concentrations of nanoparticles for 24 to 48 h. Each value represents the mean ± SE of three experiments

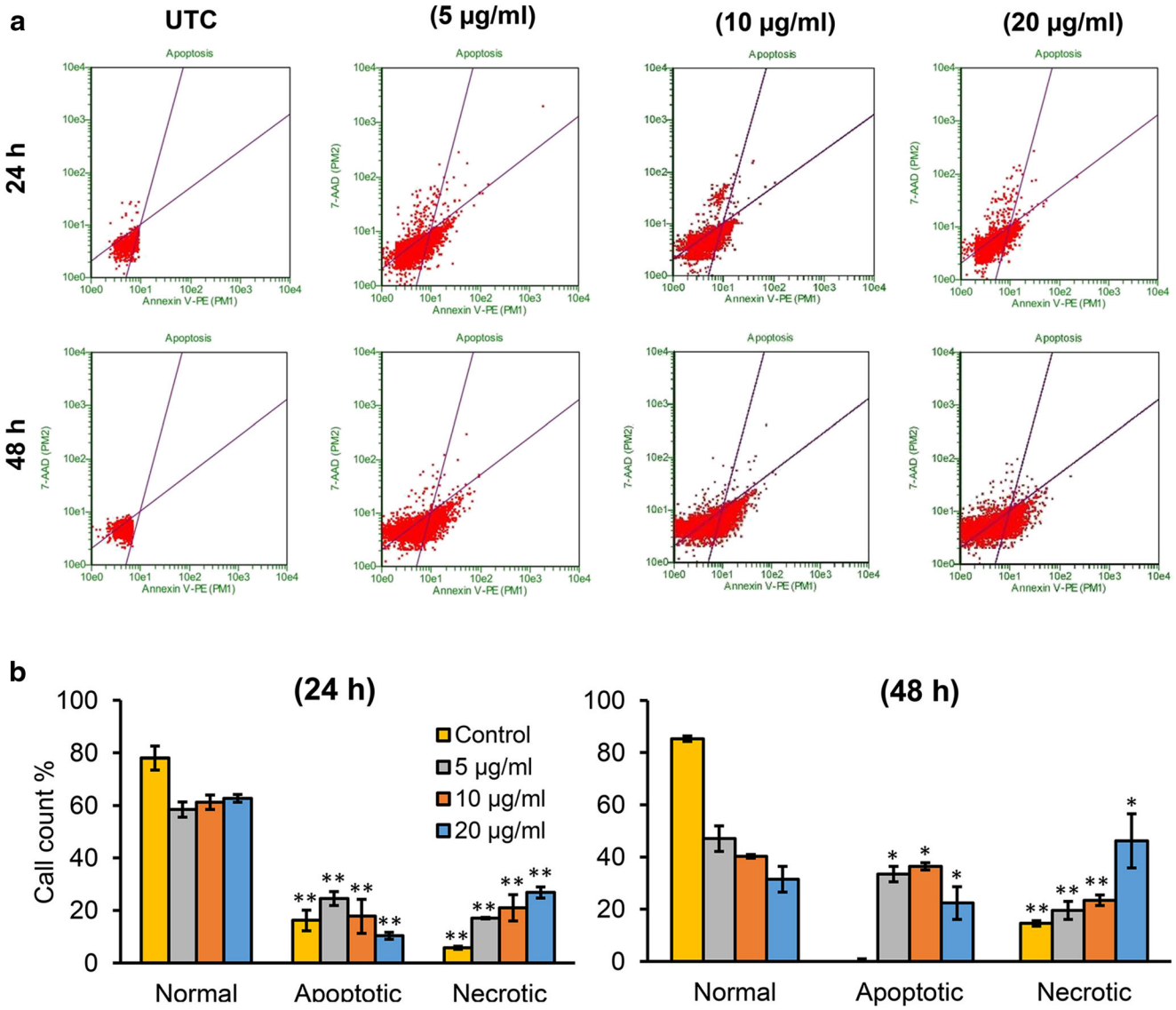

Fig. 8 Various concentrations of Bi_2O_3NPs induced apoptosis and necrosis in MCF-7 cells. **a** Annexin V-FITC and 7-AAD fluorescence were measured using flow cytometer with PI and Annexin V-FITC filters, respectively. **b** % apoptotic and necrotic cells for 24 h and 48 h. Data represent average ± SE of triplicate experiments. *p 0.05 compared with control. *$p < 0.05$ and **$p < 0.01$ vs. control

numbers of condensed chromatin in treated MCF-7 cells. Furthermore, the leakage of phosphatidylserine was increased in treated cells as compared with untreated cells. The production of intracellular ROS and changed redox status are normal physiochemical phases in MCF-7 cells. ROS may be interacting with fatty acids of plasma membrane, causing lipid peroxidation (Gaetke and Chow 2003).

Excessive generation of intracellular ROS in treated cells occurred as a consequence of nanoparticles that promote oxidative damage and apoptosis in treated cells. This was followed by increased GSH concentration, as well as SOD and CAT activities. Abudayyak et al. (2017) has pointed that Bi_2O_3NPs induced toxicity in various types of human cell lines. The oxidative stress assay consists of SOD, catalase, and GSH; these are the defense tools to eliminate the oxidative stress in the cells. Xiong et al. (2014) suggested that mitochondria play an important role in apoptosis pathways, and the loss of mitochondrial integrity may be prevented by different apoptotic markers. Bi2O3NPs weaken the mitochondrial membrane potential in MCF-7 cells. In this study, we found that cells, treated with Bi_2O_3NPs, had impaired mitochondrial membrane function, which results in high rate of apoptosis. Hüttemann et al. (2011) has reported that oxidative stress activates caspase enzymes via releasing cytochrome-c from the inter-membrane space into the cytoplasm. Our results showed caspase-3 activity and phosphatidylserine externalization, and apoptotic and necrotic cells were increased

after Bi_2O_3NP exposure in a concentration- and duration-dependent manner. These results were confirmed by fluorescence-activated cell sorting (FACS) using Annexin V-FITC and 7-AAD stains. In addition, this result showed that Bi_2O_3NPs damage the DNA, as this leads to the death of the cells. Mitochondria play a significant role in metal toxicity through inducing intracellular ROS generation (Keunen et al. 2011). Stewart et al. (2014) reported that nanoparticles increase ROS generation beyond the oxidative stress threshold of the cell, and finally resulting in apoptosis.

On the basis of the above finding, we conclude that Bi_2O_3NPs induce intracellular ROS generation and oxidative stress and provoked damage to the nuclear materials and organelles of MCF-7 cells. This study suggests that the use of Bi_2O_3NPs should be minimized because of its toxicity.

Authors' contributions Ali Alamer, Daoud Ali, Saud Alarifi, and Abdullah Alkahtane acquired and analyzed the data regarding the cytotoxicity of Bi_2O_3NPs. Mohammed AL-Zharani and Mohamed M. Abdel-Daim acquired and analyzed the data regarding physiochemical characterization of Bi_2O_3NPs and oxidative stress biomarkers. Gadah Albasher and Rafa Almeer acquired and analyzed the data regarding apoptotic markers. Abdulaziz Almalik and Ali H Alhasan contributed in writing the manuscript. Nouf K. Al-Sultan and Ali Alamer contributed in statistical analysis. Christos Stournaras, Saquib Hasnain, and Saad alkahtani were involved in the conception and design of the study and data interpretation, and critically revised the manuscript. All authors read and approved the final manuscript.

Funding The authors extend their appreciation to the International Scientific Partnership Program (ISPP) at King Saud University for funding this research work through ISPP#009.

Data availability The data generated or analyzed in this article are online and publicly available without request.

Compliance with ethical standards

Competing interests The authors declare that they have no conflict of interest.

Ethics approval and consent to participate Not applicable.

Consent to publish Not applicable.

References

Abudayyak M, Öztaş E, Arici M, Özhan G (2017) Investigation of the toxicity of bismuth oxide nanoparticles in various cell lines. Chemosphere 169:117–123

Alberts B (2008) The promise of cancer research. Science 320(5872):19. https://doi.org/10.1126/science.1158084

Bradford MM (1976) A rapid sensitive method for the quantification of microgram quantities of protein utilizing the principle of protein-dye binding. Anal Biochem 72:248–254

Chen C, Zhao KN, Masci PP, Lakhani SR, Antonsson A, Simpson PT, Vitetta L (2015) TGFβ isoforms and receptors mRNA expression in breast tumours: prognostic value and clinical implications. BMC Cancer 15:1010

Ding N, Yamashita U, Matsuoka H, Sugiura T, Tsukada J, Noguchi J, Yoshida Y (2011) Apoptosis induction through proteasome inhibitory activity of cucurbitacin D in human T-cell leukemia. Cancer 117(12):2735–2746

Doubeni C, Fedewa S, Levin T, Jensen C, Saia C, Zebrowski A, Quinn V, Rendle K, Zauber A, Becerra-Culqui T, Mehta S, Fletcher R, Schottinger J (2019) Modifiable failures in the colorectal cancer screening process and their association with risk of death. Gastroenterology 156(1):63–74

Finkel T, Holbrook NJ (2000) Oxidants, oxidative stress and the biology of ageing. Nature 408(6809):239–247

Gaetke LM, Chow CK (2003) Copper toxicity, oxidative stress, and antioxidant nutrients. Toxicology 189(1-2):147–163

He J, Li S, Shao W, Wang D, Chen M, Yin W, Wang W, Gu Y, Zhong B (2010) Activated carbon nanoparticles or methylene blue as tracer during video-assisted thoracic surgery for lung cancer can help pathologist find the detected lymph nodes. J Surg Oncol 102(6):676–682. https://doi.org/10.1002/jso.21684

Hüttemann M, Pecina P, Rainbolt M, Sanderson TH, Kagan VE, Samavati L, Lee I (2011) The multiple functions of cytochrome c and their regulation in life and death decisions of the mammalian cell: from respiration to apoptosis. Mitochondrion 11(3):369–381

Hyodo F, Chandramouli GV, Matsumoto S, Matsumoto K, Mitchell JB, Krishna MC, Munasinghe JP (2009) Estimation of tumor microvessel density by MRI using a blood pool contrast agent. Int J Oncol 35(4):797–804

Karam JA, Lotan Y, Karakiewicz PI, Ashfaq R, Sagalowsky AI, Roehrborn CG, Shariat SF (2007) Use of combined apoptosis biomarkers for prediction of bladder cancer recurrence and mortality after radical cystectomy. Lancet Oncol 8(2):128–136

Keunen E, Remans T, Bohler S, Vangronsveld J, Cuypers A (2011) Metal-induced oxidative stress and plant mitochondria. Int J Mol Sci 12(10):6894–6918

Kooti W, Servatyari K, Behzadifar M, Asadi-Samani M, Sadeghi F, Nouri B, Zare Marzouni H (2017) Effective medicinal plant in cancer treatment, part 2: review study. J Evid Based Complementary Altern Med 22(4):982–995

Novaro V, Roskelley CD, Bissell MJ (2003) Collagen-IV and laminin-1 regulate estrogen receptor α expression and function in mouse mammary epithelial cells. J Cell Sci 116(14):2975–2986

Patil D, Le TL, Bens KB, Alemozaffar M, Lay A, Pattaras J, Filson CP, Ogan K, Bilen MA, Master VA (2020) Dynamic evaluation of the modified Glasgow prognostic scale in patients with resected, localized clear cell renal cell carcinoma. Urology. S0090-4295(20)30340-X. https://doi.org/10.1016/j.urology.2020.03.024

Pradeepkumar T, and Kumar Pradeep (2018) Management of horticultural crops: Vol.11 Horticulture Science Series: In 2 Parts. New India Publishing. 601– 622

Riaz M, van Jaarsveld MT, Hollestelle A, Prager-van der Smissen WJ, Heine AA, Boersma AW, Smid M (2013) miRNA expression profiling of 51 human breast cancer cell lines reveals subtype and driver mutation-specific miRNAs. Breast Cancer Res 15(2):R33

Stewart E, Goshorn R, Bradley C, Griffiths LM, Benavente C, Twarog NR, Bahrami A (2014) Targeting the DNA repair pathway in Ewing sarcoma. Cell Rep 9(3):829–840

Strayer ME, Senftle TP, Winterstein JP, Vargas-Barbosa NM, Sharma R, Rioux RM, Janik MJ, Mallouk TE (2015) Charge transfer stabilization of late transition metal oxide nanoparticles on a layered niobate support. J Am Chem Soc 137(51):16216–16224. https://doi.org/10.1021/jacs.5b11230 Epub 2015 Dec 21

Toné S, Sugimoto K, Tanda K, Suda T, Uehira K, Kanouchi H, Samejima K, Minatogawa Y, Earnshaw WC (2007) Three distinct stages of apoptotic nuclear condensation revealed by time-lapse imaging, biochemical and electron microscopy analysis of cell-free apoptosis. Exp Cell Res 313(16):3635–3644

Valko M, Leibfritz D, Moncol J, Cronin MT, Mazur M, Telser J (2007) Free radicals and antioxidants in normal physiological functions and human disease. Int J Biochem Cell Biol 39(1):44–84

Wang C, Hu L, Poeppelmeier K, Stair PC, Marks L (2017) Nucleation and growth process of atomic layer deposition platinum nanoparticles on strontium titanate nanocuboids. Nanotechnology 28(18):185704

Xiong S, Mu T, Wang G, Jiang X (2014) Mitochondria-mediated apoptosis in mammals. Protein Cell 5(10):737–749